Clays and Clay Minerals, Vol. 38, No. 4, 373–379, 1990.

DIRECT HIGH-RESOLUTION TRANSMISSION ELECTRON MICROSCOPIC MEASUREMENT OF EXPANDABILITY OF MIXED-LAYER ILLITE/SMECTITE IN BENTONITE ROCK

JAN ŚRODOŃ

Institute of Geological Sciences, Polish Academy of Sciences
Senacka 3, 31-002 Kraków, Poland

CRISTINA ANDREOLI, FRANÇOISE ELSASS, AND MICHEL ROBERT

Station de Science du Sol INRA
Route de Saint-Cyr, 78000 Versailles, France

Abstract—Samples of mixed-layer illite/smectite were investigated from a single bentonite bed zoned with respect to expandability from 90 to 30%. Chips of natural rocks were embedded in a resin, using a procedure designed to preserve the original fabric, cut with an ultramicrotome, and observed by high-resolution transmission electron microscopy (HRTEM). These observations confirmed the X-ray powder diffraction (XRD) model of mixed-layer clays, i.e., that illite/smectite grains in natural rocks are built of mixed-layer crystals, from 1 to as many as 15 silicate layers thick (4–6 interlayers per crystal on average). These crystals are present either as individual particles (loose crystals) or, typically, they form nearly parallel face-to-face groupings called here quasi-crystals. Free fundamental smectite and illite particles as defined by Nadeau and coworkers were essentially absent.

Illite and smectite interlayer spacings were 10 and 13.5 Å, respectively. Crystal thickness and number of interlayers were measured for 35–100 mixed-layer crystals per sample. Illite/smectite expandabilities were calculated from these data in two ways: either neglecting the crystal edges or accounting for them. The former determinations agree well with XRD estimates of expandability and the latter, with expandabilities calculated from the distributions of fundamental particle thickness measured by a shadowing technique in the TEM. This result explains the systematic discrepancy between XRD and TEM measurements of illite/smectite expandability.

Key Words—Expandability, Fundamental particle, High-resolution transmission electron microscopy, Illite/smectite, Interstratification.

INTRODUCTION

Expandability (i.e., percentage of smectite layers) of mixed-layer illite/smectite minerals (I/S) is typically measured by two techniques: X-ray powder diffraction (XRD) and transmission electron microscopy (TEM). XRD models calculate diffraction patterns from mixed-layer crystals (named MacEwan crystallites by Altaner *et al.*, 1988), i.e., sets of parallel silicate 2:1 layers with illite and smectite interlayers, which are intimately mixed in random fashion or according to various patterns (see Reynolds, 1980, Figure 4.3). The best fit of the experimental data is obtained by assuming distributions of crystal size from 1 to a maximum of about 8–14 layers per mixed-layer crystal (Środoń, 1980). In current XRD models, the mixed-layer crystals are assumed to terminate on tetrahedral sheets of the external silicate layers, and expandability is defined as the percentage of smectite interlayers *within* the mixed-layer crystals (Reynolds, 1980). Consequently, the top and bottom halves of external silicate layers of a mixed-layer crystal and the cations associated with them are not taken into account by the expandability calculation.

TEM observations of finely dispersed clays reveal the presence of fundamental particles, i.e., individual 10-Å thick silicate layers (smectite) and multiple silicate layers (20, 30, 40 Å, etc.). The latter are bound together permanently by fixed cations, as evidenced by the lack of turbostratic rotations observed by selected-area electron diffraction (Nadeau *et al.*, 1984). Nadeau *et al.* (1984) identified these multiple-layer particles as illite. Expandability can thus be calculated from data on the distribution of the thickness of such fundamental particles, assuming that their edges are smectitic, which amounts to one smectite interlayer per fundamental particle (Eberl *et al.*, 1987, Eq. (1)).

A systematic discrepancy between XRD and TEM expandability measurements has been observed, the TEM values being greater (Nadeau, 1985; Eberl *et al.*, 1987). An obvious explanation of this discrepancy blames the XRD measurements for underestimating the number of smectite interlayers; tops and bottoms of mixed-layer crystals accounting for one extra smectite interlayer are omitted by the XRD modeling (Eberl and Środoń, 1988).

XRD and TEM approaches have led to different

concepts of the physical structure of the mixed-layer clays. Older XRD studies implied that mixed-layer crystals actually existed in rocks (Reynolds, 1980, par. 3.5). Students of TEM, in their most radical statement, have written that only fundamental illite and smectite particles exist in sandstones and bentonites and that the effect of interparticle diffraction between these particles, stacked on an X-ray slide, gives rise to a mixed-layering effect (Nadeau *et al.,* 1985).

High-resolution transmission electron microscopy (HRTEM) is an obvious choice for solving the outlined controversies, but first attempts have only added to the confusion: Ahn and Peacor (1986a), after studying ion-thinned samples of shales, stated that what really existed in rocks were megacrystals of smectite and illite tens of layers thick. They interpreted mixed-layering as an artifact due to the disintegration of megacrystals in the course of X-ray sample preparation. Recently, these authors withdrew their interpretation (Ahn and Peacor, 1989). Other authors, who used organic cations to expand the smectite interlayer to make it clearly distinct from the illite interlayer (Bell, 1986; Klimentidis and Mackinnon, 1986; Vali and Köster, 1986), reported mixed-layer crystals tens of layers thick. Their observations are not fully conclusive for the above controversy, because the measurements were made on clay fractions separated from the bulk rocks. It can be argued, from the fundamental particle perspective, that the observed mixed-layer crystals are artifacts of the preparation technique. Similar objection can be raised against the observations of mixed-layer crystals in the bulk rock by the ion-milling technique (Klimentidis and Mackinnon, 1986; Huff *et al.,* 1988). Drying bulk rocks without special precautions is believed to produce mixed-layering by aggregation of fundamental particles (McHardy *et al.,* 1982).

In the present study, the textures of several I/S minerals were observed in chips of natural rocks that were processed to preserve their original fabric. Furthermore, the expandabilities of these minerals were measured directly from HRTEM images and compared with XRD and TEM data.

MATERIALS AND METHODS

Samples

The five samples analyzed in this study came from a single Carboniferous bentonite bed from the Upper Silesian Coal Basin (Southern Poland). The bed was characterized from sedimentological and mineralogical standpoint by Środoń (1976). Its thickness varies from a few centimeters to several meters, and it is known from coal mines and boreholes over an area of about 100 km^2. This bentonite bed is not an original ashfall, but reworked ash, deposited in a lake with a minor (a few percent) admixture of epiclastic minerals and organic detritus. The volcanic glass was altered to clay after deposition (Środoń, 1976). Deep diagenesis followed (vitrinite reflectance of about 0.9; see Środoń, 1979). The bed is now zoned with respect to expandability from about 90% in the center to 30% at the contacts with the surrounding shales (Środoń, 1976). The five samples selected for this study came from three profiles of the bed, and they represent the whole known range of expandability.

All five samples were chips of natural bentonite rock. One of them (Ch5) was also investigated in the form of "clay cake" obtained by dispersing the rock in distilled water into a thick slurry and slowly drying it. The uppermost zone of the cake was sampled and cut perpendicularly to the sedimentation surface.

Expandabilities of I/S minerals from all samples were measured in <0.2-μm fractions by X-ray powder diffraction technique of Środoń (1980). For two samples, expandabilities calculated from TEM data by the technique of Eberl *et al.* (1987) were also available (J. Środoń, unpublished data). Chemical data for the investigated I/S minerals were reported by Środoń *et al.* (1986).

Sample preparation

The samples were processed using the technique of Tessier (1984), which was originally designed for soils to avoid aggregation artifacts due to drying. The technique was adapted by the authors for embedding harder and more compacted samples, such as bentonites. First, air-dried rock chips lying on a porous membrane were rehydrated by capillarity at a hydration potential fixed by an applied air pressure of 32 hPa (pF = 1.5). A previous agar coating of the chips ensured a homogenous rehydration from the periphery to the center of the chip and a perfect contact with the porous membrane. It preserved the sample fabric throughout the embedding process, assuring gentle changes of osmotic pressures, which minimized the changes of intra- and intercrystalline cohesion forces. This procedure also limited disaggregation artifacts related to splitting and dispersion processes, which tended to take place during more drastic modifications of the physical state of clay samples.

After rehydration, water was removed with methanol, and the methanol was removed with L. R. White resin of very low viscosity, even if compared to Spurr resin, which is more commonly used for embedding of hydrated samples.

After curing the resin, sections about 500 Å thick were cut with a diamond knife using a Reichert Ultracut E microtome and deposited on carbon and collodion-covered copper TEM grids.

Microscopy and image interpretation

HRTEM one-dimensional and bright-field lattice-fringe imaging was performed on numerous fields for each sample. The microscope was a Philips 420 STEM

working at 120 kV accelerating voltage and mounted with a W filament. The spherical aberration coefficient of the objective was Cs = 1.65.

For the 120-kV potential, the wavelength of the electrons, determined by the relativisitic relation, is $\lambda = 3.35 \times 10^{-3}$ nm. The Scherzer defocalization is $\Delta z = 1.25\sqrt{Cs\lambda} \approx 100$ nm. In symmetrical beam conditions, the applied 40-μm objective aperture selects for the image formation the direct beam and the diffracted beams corresponding to lattice periodicities >3.5 Å. Lattice periodicities of interest, i.e., ≥10 Å, were thus largely included. For phyllosilicates, 001 reflections from particles oriented with (*hk*0) parallel to the electron beam were in a proper Bragg diffraction position.

The images observed by electron microscopy are, to first approximation, related to the corresponding electron diffraction patterns through their Fourier transforms (Buseck and Iijima, 1974). The orientation with respect to the electron beam can be checked either by electron diffraction patterns or by the contrast in the images. In the proper orientation, electron diffraction patterns display symmetrical dots of equal intensities along the (001) row, whereas the lattice fringes of the silicate layers perpendicular to the stacking direction of the sheets show a maximum of contrast.

The interpretation of the images of phyllosilicates can be either intuitive and restricted to measuring stacking periodicities (Lee *et al.*, 1985; Bell, 1986; Ahn and Peacor, 1986a, 1986b; Huff *et al.*, 1988) or based on earlier theoretical work (Iijima and Buseck, 1978; O'Keefe *et al.*, 1978; Veblen, 1983a, 1983b; Spinnler *et al.*, 1984; Klimentidis and Mackinnon, 1986). Amouric *et al.* (1981) performed extensive calculations of image contrast in micas. More recently, Guthrie and Veblen (1989) completed HRTEM simulations for mixed-layer illite/smectites.

In ultrathin sections, such as investigated in this study, very thin (≤150 Å) zones of properly oriented layers are examined, due to bending of the particles or to their position at the edge of the section. Such thin zones of low atom density, implying low scattering, can be considered weak phase objects, and the kinematic theory of electron-matter interaction can be applied. It implies that layers having high electrostatic potential appear dark, and the interlayer spaces with low electrostatic potential appear light on the microscope screen or on photographic prints.

Because the microscope is not perfect, the spherical aberration of the objective lens must be taken into account. If the objective current is varied, the focus also changes, and this change (Δz) introduces an additional phase delay, which is proportional to Δz.

For the purpose of the present work, the optimal conditions required an underfocus between 1000 and 1500 Å for imaging both 10 and 14 Å simultaneously, with a good transfer efficiency in the microscope. Zero focus was obtained on the carbon support. The selected defocus took into account the thickness of the section and the position of the object in the section, the minimum defocus of 1000 Å being the Scherzer defocus.

A magnification of 105,000× was routinely applied. Several photographs of each sample were taken. Measurements of the images were made directly from the negatives by means of a Peak 10× magnifying glass and a light table. Crystal thickness was measured between the centers of external fringes (Figure 1). Artifacts due to physical disruption during microtoming appeared as wide, eye-shaped holes, and were easy to avoid.

OBSERVATIONS OF IMAGES AND THE TECHNIQUE OF EXPANDABILITY MEASUREMENT

The nomenclature ofTessier and Pedro (1985) is used here to describe the layer arrangements observed in the rocks under study. Two levels of clay organization were noted. The smallest clay particles consisted of individual layers or, more commonly, sets of layers of strictly parallel orientation. In this article, they are called crystals and are regarded as the coherent scattering domains from the point of view of XRD. Crystals were observed as individual particles, designated here as loose crystals (Figure 1A), or they formed nearly parallel face-to-face groupings (Figure 1B)—so called quasi-crystals. The latter are presumably identical with the "smectite megacrystals" of Ahn and Peacor (1986a).

The loose crystals were typically only a few layers thick and a few hundreds of Ångstroms long. The crystals constituting the quasi-crystals were commonly thicker than the loose crystals (as many as 15 layers). The quasi-crystals were hundreds of Ångstroms thick and thousands of Ånstroms long. Most of the rock mass consisted of quasi-crystals; loose crystals accounted for not more than 10% of the total mass. The clay cake sample consisted of loose crystals or small quasi-crystals built of only a few crystals. Big quasi-crystals, characteristic of the natural rocks, were lacking.

Most crystals, both outside and inside quasi-crystals, exhibited variable layer spacings, very much like these observed in ion-thinned specimens by Ahn and Peacor (1986a) and Huff *et al.* (1988). Some crystals having identical layer spacing were noted, mostly in sample 2M9 containing the largest smectite percentage (large spacing) and sample R62 containing the largest illite percentage (small spacing). In both materials, the thickest measured crystals having identical spacings contained eight interlayers. The values of interlayer spacings, obtained by dividing the total crystal thickness by the number of interlayers, were 13.5 Å for sample 2M9 and 10 Å for sample R62.

Accepting the above interlayer spacings as smectite (D_S) and illite (D_I) spacings, respectively, expandability was estimated from the data obtained from HRTEM photographs, i.e., the crystal thickness and the number

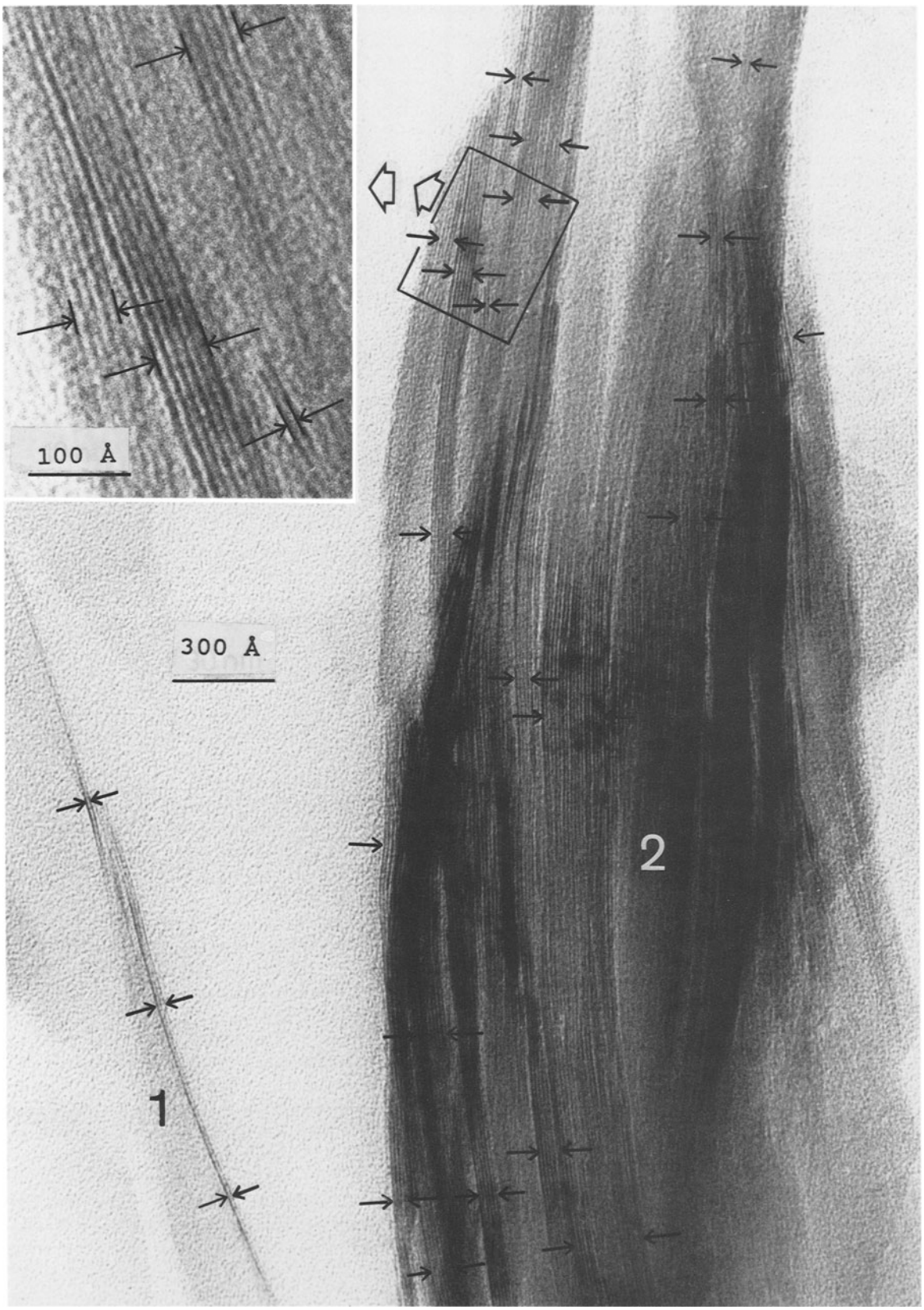

Figure 1. Sample Ch5. Lattice-fringe images of (1) loose crystal and (2) quasi-crystal. Crystal cross-sections measured in this photograph are marked with arrows.

https://doi.org/10.1346/CCMN.1990.0380406 Published online by Cambridge University Press

Table 1. Data obtained from high-resolution transmission electron microscope images of illite/smectite samples and expandabilities (%) calculated from these data and estimated by other techniques.

Sample	T (Å)	N	No	N/No	Exp_{MIN}	Exp_{MAX}	Exp_{XRD}	Exp_{TEM}
2M9	3827	293	48	6	87	89	88	—
2M3A	5711	458	79	6	71	75	70	—
R49	1930	163	35	5	53	61	50	—
Ch5	4518	397	65	6	39	48	39	45
Ch5-cake	2321	206	47	4	36	47	39	45
R62	4967	450	106	4	30	43	29	37

T = total measured thickness of crystal cross-sections; N = total number of interlayers in measured crystal cross-sections; No = number of measured crystal cross-sections; N/No = average number of interlayers in measured crystals; Exp_{MIN} = expandability calculated from Eq. (1) in text; Exp_{MAX} = expandability calculated from Eq. (2) in text; Exp_{XRD} = expandability measured by X-ray powder diffraction (XRD); Exp_{TEM} = expandability calculated from transmission electron microscopic (TEM) data (from distribution of thickness of fundamental particles).

of interlayers in a crystal. For statistical reasons, numerous crystals were measured. The data were summed to give a "total" measured thickness (T) and a "total" number of measured interlayers (N), and expressed as follows:

$$T = N_S D_S + N_I D_I \quad \text{and} \quad N = N_S + N_I,$$

where N_S and N_I are total numbers of smectite and illite interlayers, respectively. Thus,

$$N_S = T - ND_I/D_S - D_I.$$

Expandability *within* the crystals (Exp_{MIN}), i.e., the percentage of smectite interlayers was then calculated:

$$Exp_{MIN} = N_S(100\%)/N = (T - ND_I)(100\%)/N(D_S - D_I). \quad (1)$$

Eq. (1) gives an expandability value that should correspond to the XRD measurement, because in this calculation, like in the XRD models (see Introduction) the crystal edges were neglected. Eq. (1) can be modified to account for the crystal edges, if an assumption is made about their nature. In the following equation, the edges are assumed to be smectitic, meaning that one extra smectite interlayer per crystal (two edges) must be added to the calculations:

$$Exp_{MAX} = (T + NoD_S) - (N + No)D_I \div (N + No)(D_S - D_I). \quad (2)$$

"No" is the number of crystals measured for a given sample. The assumption of smectitic crystal edges was made to obtain a HRTEM measure of expandability (Exp_{MAX}) compatible with TEM-based estimates. In both cases, the condition of one smectite layer per fundamental particle was fulfilled (see Introduction).

RESULTS AND DISCUSSION

All sharp crystal cross-sections were measured. An example of the measurement is presented in Figure 1. The data and the calculations of expandability from Eqs. (1) and (2) are given in Table 1, along with XRD expandabilities and two available TEM expandabilities (J. Środoń, unpublished data). Average crystal thickness (N/No) is given also.

The agreement between Exp_{MIN} and Exp_{XRD} is remarkable. The differences do not exceed 3%, i.e., they are within the error involved in XRD expandability determination (Środoń, 1980). Sample R49, for which the fewest crystals were available for measurement (Table 1), showed the largest discrepancy between Exp_{MIN} and Exp_{XRD}. Significant differences in expandability (as much as 20%) between quasi-crystals were observed, and only by averaging all measurements from several photographs were numbers close to the XRD estimates achieved. The problem of sample heterogeneity deserves further study.

Limited data (three measurements) indicate that the agreement between Exp_{MAX} and Exp_{TEM} is as good (2–6% difference) as for the pair Exp_{MIN}-Exp_{XRD}. This result is not yet a hard proof that the crystal edges are smectitic, but it indicates that the assumption of smectitic edges of mixed-layer crystals (this article) and the assumption of smectitic surfaces of fundamental particles (Nadeau *et al.*, 1984) leads to a similar estimate of expandability, larger than the XRD estimate. The discrepancy between Exp_{MIN} and Exp_{MAX} increased for more illitic compositions, in agreement with the greater discrepancy between Exp_{XRD} and Exp_{TEM} in this expandability range (Eberl and Środoń, 1988).

The range of crystal thickness measured in this study spreads from a monolayer to about 15 layers per crystal, which corresponds very well to the range estimated previously from the computer modeling of XRD patterns (Reynolds, 1980; Środoń, 1980). The average crystal thickness (N/No in Table 1) is 4–6 interlayers per crystal and does not seem to evolve with progressing illitization. The measured value is identical with the average thickness of Ca-smectite crystals in suspension, calculated from negative absorption measurements (Quirk and Aylmore, 1971).

Sample Ch5, when investigated as clay cake, gave smaller average crystal thickness, smaller Exp_{MIN}, but Exp_{MAX} close to the natural rock (Table 1). Such differences may have resulted either from disruption of

https://doi.org/10.1346/CCMN.1990.0380406 Published online by Cambridge University Press

larger crystals along smectitic interlayers or from fractionation of crystals and quasi-crystals during sedimentation (the clay cake was sampled at the top surface).

SUMMARY AND CONCLUSIONS

The results of this HRTEM study can be summarized as follows:

1. Under the applied experimental conditions, the texture of the sample undoubtedly shrank due to the decrease of expandability of smectite layers in alcohol compared with water, but the general fabric of the samples was preserved. I/S observed directly in a bentonite rock, consisted of crystals ranging from a monolayer to about 15 layers thick. Most crystals were aggregated into quasi-crystals, which were hundreds of Ångstroms thick and thousands of Ångstroms long.
2. Most of the crystals were mixed-layer crystals (i.e., they contained mixed illite and smectite interlayers), and their measured thicknesses agreed well with XRD estimates of the mixed-layer crystal size (the size of the coherent scattering domain). Loose fundamental particles (Nadeau *et al.*, 1985) were very rare. Thus, at least for the bentonites examined in this investigation, illitization of smectite took place only within mixed-layer crystals. Fundamental particles appear to have formed by the swelling of mixed-layer crystals along the smectite interlayers during TEM sample preparation, which involved a severe dispersion process (as small as 1 mg clay per 40 ml H_2O).
3. The smectite layers of the investigated samples retained a stable layer spacing of about 13.5 Å, as indicated by the results of calculations of expandability using this value. These HRTEM results agreed well with the XRD estimates, if edges of crystals were neglected, and with the TEM estimates, if the edges were accounted for, thereby explaining the systematic discrepancy between the latter two techniques. The result is consistent with the earlier calculation of "the short stack" effect by Eberl and Środoń (1988).

ACKNOWLEDGMENTS

We thank D. D. Eberl for a review of the initial manuscript. J.Ś. acknowledges support from The Polish Academy of Sciences Program CPBP 03.04 and thanks INRA for supporting his visit to Versailles, during which most of this study was made.

REFERENCES

Ahn, J. H. and Peacor, D. R. (1986a) Transmission and analytical electron microscopy of the smectite-to-illite transition: *Clays & Clay Minerals* **34,** 165–179.

Ahn, J. H. and Peacor, D. R. (1986b) Transmission electron microscope data for rectorite: Implications for the origin and structure of "fundamental particles": *Clays & Clay Minerals* **34,** 180–186.

Ahn, J. H. and Peacor, D. R. (1989) Illite/smectite from Gulf Coast anales: A reappraisal of transmission electron microscope images: *Clays & Clay Minerals* **37,** 542–546.

Altaner, S. P., Weiss, C. A., Jr., and Kirkpatrick, R. J. (1988) Evidence from ^{29}Si NMR for the structure of mixed-layer illite/smectite clay minerals: *Nature* **331,** 699–702.

Amouric, M., Mercuriot, G., and Baronnet, A. (1981) On computed and observed HRTEM images of perfect mica polytypes: *Bull. Mineral.* **104,** 298–313.

Bell, T. E. (1986) Microstructure in mixed-layer illite/smectite and its relationship to the reaction of smectite to illite: *Clays & Clay Minerals* **34,** 146–154.

Buseck, P. R. and Iijima, S. (1974) High resolution electron microscopy of silicates: *Amer. Mineral.* **59,** 1–21.

Eberl, D. D. and Środoń, J. (1988) Ostwald ripening and interparticle-diffraction effects for illite crystals: *Amer. Mineral.* **73,** 1335–1345.

Eberl, D. D., Środoń, J., Lee, M., Nadeau, P. H., and Northrop, H. R. (1987) Sericite from the Silverton caldera, Colorado: Correlation among structure, composition, origin, and particle thickness: *Amer. Mineral.* **72,** 914–934.

Guthrie, G. D. and Veblen, D. R. (1989) High-resolution transmission electron microscopy of mixed-layer illite/smectite: Computer simulations: *Clays & Clay Minerals* **37,** 1–11.

Huff, W. D., Whiteman, J. A., and Curtis, C. D. (1988) Investigation of K-bentonite by X-ray powder diffraction and analytical transmission electron microscopy: *Clays & Clay Minerals* **36,** 83–93.

Iijima, S. and Buseck, P. R. (1978) Experimental study of disordered mica structures by high-resolution electron microscopy: *Acta Crystallogr.* **34,** 709–719.

Klimentidis, R. E. and Mackinnon, I. D. R. (1986) High-resolution imaging of ordered mixed-layer clays: *Clays & Clay Minerals* **34,** 155–164.

Lee, J. H., Ahn, J. H., and Peacor, D. R. (1985) Textures in layered silicates: Progressive changes through diagenesis and low-temperature metamorphism: *J. Sed. Petrol.* **55,** 532–540.

McHardy, W. J., Wilson, M. J., and Tait, J. M. (1982) Electron microscope and X-ray diffraction studies of filamentous illitic clay from sandstones of the Magnus field: *Clay Miner.* **17,** 23–39.

Nadeau, P. H. (1985) The physical dimensions of fundamental clay particles: *Clay Miner.* **20,** 499–514.

Nadeau, P. H., Wilson, M. J., McHardy, W. J., and Tait, J. M. (1984) Interparticle diffraction: A new concept for interstratified clays: *Clay Miner.* **19,** 757–769.

Nadeau, P. H., Wilson, M. J., McHardy, W. J., and Tait, J. M. (1985) The conversion of smectite to illite during diagenesis: Evidence from some illitic clays from bentonites and sandstones: *Mineral. Mag.* **49,** 393–400.

O'Keefe, M. A., Buseck, P. R., and Iijima, S. (1978) Computed crystal structure images for high resolution electron microscopy: *Nature* **274,** 322–324.

Quirk, J. P. and Aylmore, L. A. G. (1971) Domains and quasi-crystalline regions in clay sytems: *Soil. Sci. Soc. Amer. Proc.* **35,** 652–654.

Reynolds, R. C., Jr. (1980) Interstratified clay minerals: in

Crystal Structures of Clay Minerals and their X-ray Identification, G. W. Brindley and G. Brown, eds., Mineralogical Society, London, 249–303.

Spinnler, G. E., Self, P. G., Iijima, S., and Buseck, P. R. (1984) Stacking disorder in clinochlore chlorite: *Amer. Mineral.* **69,** 252–263.

Środoń, J. (1976) Mixed-layer smectite/illites in the bentonites and tonsteins of the Upper Silesian Coal Basin: *Prace Mineral.* **49,** 1–84.

Środoń, J. (1979) Correlation between coal and clay diagenesis in the Carboniferous of the Upper Silesian Coal Basin: in *Proc. Int. Clay Conf., Oxford, 1978,* M. M. Mortland and V. C. Farmer, eds., Elsevier, Amsterdam, 251–260.

Środoń, J. (1980) Precise identification of illite/smectite interstratifications by X-ray powder diffraction: *Clays & Clay Minerals* **28,** 401–411.

Środoń, J., Morgan, D. J., Eslinger, E. V., Eberl, D. D., and Karlinger, M. R. (1986) Chemistry of illite/smectite and end-member illite: *Clays & Clay Minerals* **34,** 368–378.

Tessier, D. (1984) Etude experimentale de l'organisation des materiaux argileux: Dr. Science thesis, Univ. Paris VII, INRA publ., 361 pp.

Tessier, D. and Pedro, G. (1985) Mineralogical characterization of 2:1 clays in soils: Importance of the clay texture: in *Proc. Int. Clay Conf., Denver, 1985,* L. G. Schultz, H. van Olphen and F. A. Mumpton, eds., The Clay Minerals Society, Bloomington, Indiana, 78–84.

Vali, H. and Köster, H. M. (1986) Expanding behaviour, structural disorder, regular and random irregular interstratification of 2:1 layer-silicates studied by high-resolution images of transmission electron microscopy: *Clay Miner.* **21,** 827–859.

Veblen, D. R. (1983a) Evolution and crystal chemistry of the sodium mica wonesite: *Amer. Mineral.* **68,** 554–565.

Veblen, D. R. (1983b) Microstructures and mixed layering in intergrown wonesite, chlorite, talc, biotite, and kaolinite: *Amer. Mineral.* **68,** 566–580.

(Received 25 April 1989; accepted 20 March 1990; Ms. 1909)